Microscopic and Stochastic Simulations of Oscillations in a Simple Model of Chemical System

A. L. Kawczyński,* J. Gorecki, and B. Nowakowski

Institute of Physical Chemistry, Polish Academy of Sciences, Kasprzaka 44/52, 01-224 Warsaw, Poland

Received: January 7, 1998

In this paper we study the influence of internal fluctuations on a simple, but realistic model of a chemical system exhibiting oscillatory behavior. The results of molecular dynamics and simulations of the master equation are presented. The period of oscillations and the dynamics of the system obtained in these simulations are in agreement with phenomenology. Two types of fluctuations seem to appear in the simulations: short time scale fluctuations related to stochasticity of elementary reactions and long time scale fluctuations which correspond to random motion of trajectories in the phase space.

I. Introduction

Phenomenological kinetics satisfactorily describe ideally stirred, macroscopic, isothermal, close-to-equilibrium chemical systems containing a large number of molecules Ω. The description of such systems is based on two fundamental assumptions. First, collisions between molecules in the system are random. Next, reactive collisions are rare enough that nonreactive collisions are able to destroy possible correlations between reactive molecules, so that the system remains homogeneous. Global fluctuations of concentrations, which are of order $\Omega^{1/2}$, are neglegible in such systems. However, internal fluctuations can play an important role in far-from-equilibrium macroscopic, isothermal chemical systems which exhibit nonlinear phenomena such as bistability, excitability, simple and complex periodic oscillations, and deterministic chaos.[1,2] From the very begining of experimental studies on chemical oscillations, it became clear that fluctuations in such systems strongly affect their dynamic behavior.[3] A spontaneous appearance of inhomogeneities after switching off stirring in previously well-mixed reaction mixtures and strong influence of the stirring rate on the character of oscillations of concentrations in various chemical systems have been observed. For example, in the Belousov−Zhabotinsky (B-Z) reaction, periodic (regular) oscillations appear only at large stirring rates, whereas at small stirring rates the system oscillates in an irregular way.[3,4] The target patterns appear in thin layers of the B-Z system with ferroin as catalyst and bromomalonic acid as the organic compound.[5] The appearance of such patterns can be explained on the basis of local fluctuations.[6]

The simplest way to introduce fluctuations is the Langevin approach, in which noise terms are inserted directly into phenomenological equations.[7] Amplitudes of the noise obey the fluctuation−dissipation theorem.[8] A more rigorous approach is based on the master equation (ME) which, using "birth−death" processes, describes an evolution of a probability that a system contains a given number of molecules for each reagent.[2,7,8] The most fundamental method is provided by molecular dynamics (MD), which gives a detailed description of the behavior of all molecules composing a system (in the clasical mechanics, the momenta and the positions of all molecules).[9] The simplest technique which utilizes this approach is molecular dynamics of reactive hard spheres.[10] Other MD techniques are known which use a continuous potential of interaction between pairs of molecules (like the Lennard-Jones one),[10,11] but these methods are much less efficient than the MD of reactive hard spheres we use in this paper. If this method is applied for thermoneutral reactions, then all colllisions (reactive as well as nonreactive) between molecules are treated as elastic ones.

At the moment there is no hope to describe fluctuations in any real, macroscopic system using the ME or MD approaches. To this aim one has to reduce the size of the system to so-called mezoscopic scale. Moreover, a constructed reaction scheme should allow for significant simplification of numerical calculations. On the other hand, for the mesoscopic systems the phenomenological description must be modified by taking into account fluctuations in concentrations, which lead to Langevin-type kinetic equations. It is only in the thermodynamic limit that the average values of concentrations obtained from the ME and MD converge to phenomenological values.

In this paper we are concerned with comparisons between the MD and ME as well as the phenomenological approach for a chemical model, which allows for a consistent description. Whereas there are no problems in simulations of reactions of any order in the master equation approach,[2] there is a strong limitation in microscopic simulations using hard-sphere chemistry, because only bimolecular reactions can be simulated in the direct way. The known models for trimolecular reactions of hard spheres are artificial. Moreover, it would be more realistic if the reaction scheme consisted only of elementary reactions, excluding autocatalytic ones. Such a model is constructed in this paper and it is applied to describe simple periodic oscillations close and far from the Hopf bifurcation. The model is versatile enough to deal with an excitability, and its simpler version has been used to describe a bistability.[12−14] We present and discuss the results of numerical simulations of this system using the ME and MD approaches. To our knowledge there are only a limited number of papers in which chemical oscillations are studied at both microscopic and stochastic levels for the same system. A summary of results is presented in a recent review paper,[15] and simulations of nonlinear phenomena in a thermochemical system are given in refs 16−19.

S1089-5639(98)00711-7 CCC: $15.00
Published on Web 08/15/1998

The paper is organized as follows: section II introduces the phenomenological model; in section III we describe the methods of simulations; section IV contains the results; and in section V we compare and discuss them.

II. Phenomenological Model

The model consists of the following elementary (bimolecular) reactions:

$$\mathrm{R} + \mathrm{S} \underset{k_{-1}}{\overset{k_1}{\rightleftharpoons}} \mathrm{V} + \mathrm{S} \tag{1}$$

$$\mathrm{V} + \mathrm{E} \underset{k_{-2}}{\overset{k_2}{\rightleftharpoons}} \mathrm{X} + \mathrm{S} \tag{2}$$

$$\mathrm{X} + \mathrm{S} \xrightarrow{k_3} \mathrm{E} + \mathrm{U} \tag{3}$$

$$\mathrm{X} + \mathrm{V} \underset{k_{-4}}{\overset{k_4}{\rightleftharpoons}} \mathrm{Y} + \mathrm{S} \tag{4}$$

$$\mathrm{V} + \mathrm{S} \underset{k_{-5}}{\overset{k_5}{\rightleftharpoons}} \mathrm{U} + \mathrm{S} \tag{5}$$

The scheme is a modification of the model of an open chemical system with a catalytic (enzymatic) reaction, inhibited by an excess of its reactant V. Reactant V is transformed to the product U with E as the catalyst (steps 2 and 3). This part of the scheme is the well-known Langmuir−Hinshelwood mechanism of catalytic reactions (or the Michaelis−Menten kinetics for enzymatic reactions). Step 4 is the inhibition of the Langmuir−Hinshelwood mechanism (or the Michaelis−Menten scheme) by an excess of reactant V. It is noteworthy that many enzymes are inhibited by their reactants, and therefore the above scheme is a realistic one. Moreover, reactant V is transformed directly to product U in step 5. It is assumed, that S is a solvent, whose concentration is maintained constant. The system is open, due to step 1, in which reactant V is produced from reagent R, whose concentration is also maintained constant.

According to the mass action law, the behavior of the system is described by five kinetic equations for *V*, *U*, *E*, *X*, and *Y*, but it is easy to notice that $E(t) + X(t) + Y(t) = E_0$ is constant and it is the first integral of the system. Therefore, one of the variables *E*, *X*, or *Y* can be calculated if two others are known, and the dynamics of the system is described by four kinetic equations only.

In order to compare the phenomenological behavior with ME and MD simulations, the analysis of the kinetic equations for four variables is necessary. These equations have the form:

$$\mathrm{d}V/\mathrm{d}t = k_1RS - k_{-1}VS - k_2VE + k_{-2}XS - k_4VX + k_{-4}(E_0 - E - X)S - k_5VS + k_{-5}US \tag{6}$$

$$\mathrm{d}U/\mathrm{d}t = k_3XS + k_5VS - k_{-5}US \tag{7}$$

$$\mathrm{d}E/\mathrm{d}t = -k_2VE + (k_{-2} + k_3)XS \tag{8}$$

$$\mathrm{d}X/\mathrm{d}t = k_2VE - (k_{-2} + k_3)XS - k_4VX + k_{-4}(E_0 - E - X)S \tag{9}$$

where, for convenience, the designations of the reagents in italics are used to denote their concentrations because this notation does not cause any misunderstandings.

To make our microscopic as well as stochastic simulations efficient, chosen values of the rate constants have to ensure that all reactions occur at similar time scale. Also, ratios of the concentrations of all reagents must remain in three orders of magnitude.

In the sequel we will use k_2 as a control parameter. It is easy to see that eqs 6−9 have only one stationary state with the coordinates:

$$V_s = R/K_1 \tag{10}$$

$$U_s = \frac{k_3E_0SR}{k_2k_{-5}(k_2(R^2/(K_1K_4) + RS) + K_1S^2(k_{-2} + k_3)} + \frac{R}{K_1K_5} \tag{11}$$

$$E_s = \frac{E_0S^2(k_{-2} + k_3)}{(R^2/(K_1{}^2K_4) + RS/K_1)k_2 + S^2(k_{-2} + k_3)} \tag{12}$$

$$X_s = \frac{E_0SRk_2}{(R^2/(K_1K_4) + RS)k_2 + K_1S^2(k_{-2} + k_3)} \tag{13}$$

where $K_i = k_{-i}/k_i$ for $i = 1$, 4, and 5. The *V* coordinate of the stationary state does not depend on k_2, the *U* and *X* coordinates grow with k_2, whereas the *E* coordinate decreases with k_2. For an appropriate choice of the rate constants and the concentrations of *S*, *R*, and E_0, the system of eqs 6−9 exhibit the Hopf bifurcation at a critical value of k_2. In particular, in the case where the other parameters are equal to $S = 0.1$, $R = 0.5$, $E_0 = 0.2$, and $k_1 = 0.1$, $k_{-1} = 0.12$, $k_{-2} = 0.1$, $k_3 = 3.9$, $k_4 = 1.0$, $k_{-4} = 4.0$, $k_5 = 0.1$, and $k_{-5} = 0.1$, the Hopf bifurcation occurs at $k_2 \approx 5.914$. For a broad range of k_2 the characteristic equation for the stationary state has two negative real eigenvalues and two complex ones. It may be checked that behind the Hopf bifurcation the shape and stability of the limit cycle strongly depend on the value of k_2. For $k_2 = 8.0$, we have a large, strongly attractive limit cycle (see Figure 1B), whereas, if $k_2 = 6.0$, the limit cycle is inside the previous one, and it is much smaller and less attractive (see Figure 1A). Nevertheless, the periods of both limit cycles are almost equal ($T_{ph} = 640$ for $k_2 = 6.0$ and $T_{ph} = 653$ for $k_2 = 8.0$). As can be seen from Figure 1, for $k_2 = 8$ the trajectory initialized away from the limit cycle approaches it after three to four loops, whereas for $k_2 = 6$ it attains the limit cycle after several dozen loops. Therefore, for $k_2 = 8$ one can expect a much smaller influence of fluctuations as compared with $k_2 = 6$. Notice that oscillations of the concentrations of reagents in the case of the small limit cycle (for $k_2 = 6$) are sufficiently large to be observed in ME and MD simulations in which only limited numbers of molecules can be used.

Usually, the total concentration of the catalyst (or the enzyme) E_0 is much smaller than the concentrations of the reactant V and the product U. In this case one can separate scales of time, in which the concentrations of the reagents change. The variables *E* and *X* become then fast variables, whereas *V* and *U* are the slow ones. In such a case, one can reduce the number of variables because, according to the Tikhonov theorem,[20] the fast variables in a slow time scale are equal to their quasi-stationary values. Then the behavior of the reduced system can be described by two kinetic equations for *V* and *U* only. For the values of the parameters given above and $k_2 = 8$, the limit cycle of the reduced system is close to the projection of the limit cycle calculated from the full model, whereas for $k_2 = 6$ it is much larger and close to the limit cycle for $k_2 = 8$.

Moreover, the limit cycle for the reduced system with $k_2 = 6$ becomes as attractive as the limit cycle for the full model with $k_2 = 8$.

III. Methods of Simulations

In the ME approach,[2,7,8] the dynamics of a chemical system is represented by a random walk in the configuration space, in which coordinates are given by populations of molecules. A state of the system (1)−(5) is described by the probability distribution $P(N_V,N_U,N_E,N_X,t)$ of finding a given number $\{N_V,N_U,N_E,N_X\}$ of the molecules at time t. The evolution of $P(N_V,N_U,N_E,N_X,t)$ is governed by the following master equation

$$\partial P/\partial t = \kappa_1 N_R N_S P(N_V - 1,N_U,N_E,N_X,t) + \kappa_{-1}(N_V + 1)N_S P(N_V + 1,N_U,N_E,N_X,t) + \kappa_2(N_V + 1)(N_E + 1)P(N_V + 1,N_U,N_E + 1,N_X - 1,t) + \kappa_{-2}(N_X + 1)N_S P(N_V - 1,N_U,N_E - 1,N_X + 1,t) + \kappa_3(N_X + 1)N_S P(N_V,N_U - 1,N_E - 1,N_X + 1,t) + \kappa_4(N_V + 1)(N_X + 1)P(N_V + 1,N_U,N_E,N_X + 1,t) + \kappa_{-4}(N_{E_0} - N_E - N_X + 1)N_S P(N_V - 1,N_U,N_E,N_X - 1,t) + \kappa_5(N_V + 1)N_S P(N_V + 1,N_U - 1,N_E,N_X,t) + \kappa_{-5}(N_U + 1)N_S P(N_V - 1,N_U + 1,N_E,N_X,t) - \nu(N_V,N_U,N_E,N_X)P(N_V,N_U,N_E,N_X,t) \quad (14)$$

where

$$\nu(N_V,N_U,N_E,N_X) = \kappa_1 N_R N_S + \kappa_{-1} N_V N_S + \kappa_2 N_V N_E + (\kappa_{-2} + \kappa_3)N_X N_S + \kappa_4 N_X N_V + \kappa_{-4}(N_{E_0} - N_E - N_X)N_S + \kappa_5 N_V N_S + \kappa_{-5} N_U N_S \quad (15)$$

The master equation expresses the rate of change of a probability of a state $\{N_V,N_U,N_E,N_X\}$ as a balance of the "birth" and "death" processes. The "birth" term is formed by the positive components of the right-hand side of (14). It describes an increase of probability of a given state due to transitions from other states, after one of chemical processes (1)−(5) is performed. Consequently, the last component of the right-hand side of (14) is a "death" term, describing escape from this state to other points of the configuration space, corresponding to different populations of molecules. ν is a total rate of escape from the configuration $\{N_V,N_U,N_E,N_X\}$. The components of sum (15) represent the rates of reactive collisions, corresponding to reactions 1−5. The coefficients κ_i are related to the phenomenological rate constants of reactions 1−5 by $\kappa_i = k_i/\Omega$, where Ω is a volume of the system. This relation ensures that the phenomenological eqs (6)−(9) can be recovered from the master equation in the limit $\Omega \to \infty$, as the equations for the average concentrations $\langle N_\alpha/\Omega\rangle$. The master equation (14) gives fluctuations of the global populations of the species, so it applies to the homogeneous system, without local effects.

Exact solutions of the master equations exist only for some simple systems,[8,21] because the discrete form of these equations is inconvenient for the analytical treatment. For systems of a large volume this discreteness becomes less important, and the ME can be expressed in terms of continuum variables N_α/Ω, i.e., concentrations. This transformation yields the multivariable Fokker−Planck equation,[2,7,8] the form of which allows for a physical interpretation. Terms involving the first derivatives with respect to concentrations are related to the deterministic dynamics. Terms with the second derivatives describe dispersion of deterministic states, due to internal fluctuations in the system. The fluctuation terms are of the order $1/\Omega$; therefore, as the volume of the system increases, the deterministic drift prevails over the diffusive spread and the evolution of the system approaches the phenomenological dynamics. However, close to the Hopf bifurcation fluctuations play an important role even for systems with large volumes.

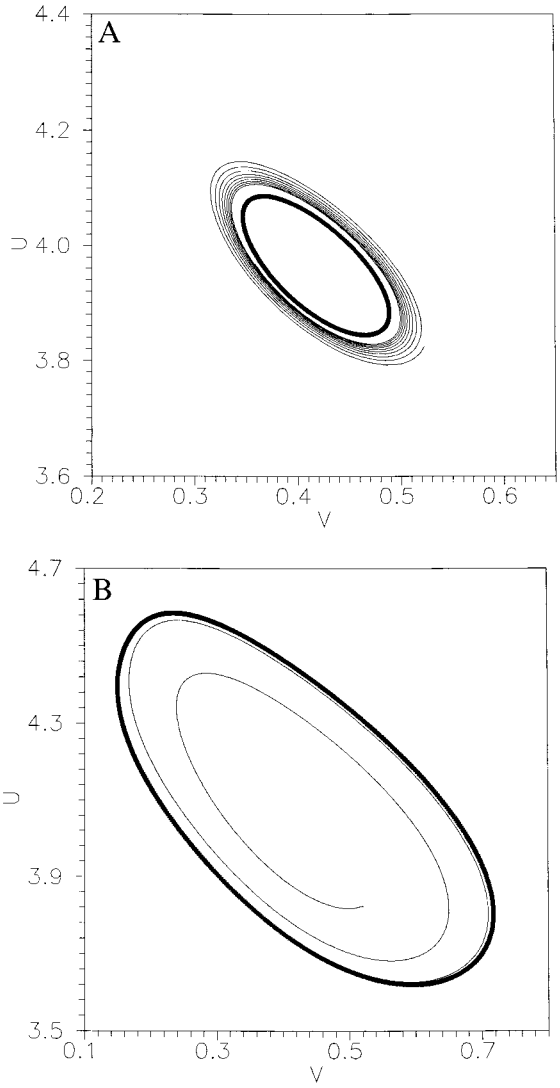

Figure 1. Projections of the phenomenological limit cycles (the thick line) on $V \times U$ plane. The thin lines show trajectories converging to the cycles: (A) corresponds to $k_2 = 6$ and (B) $k_2 = 8$. The difference in rates of the convergence is clearly seen.

On the other hand, the form (14) of the ME, involving discrete numbers N_α for populations of the species, allows for numerical simulations. We have performed simulations of the stochastic dynamics of the system applying the method of Gillespie,[22] which generates a random trajectory according to the following algorithm. Let us assume, that the system at an instant t is in a state $\{N_V,N_U,N_E,N_X\}$. In the first step, a waiting time τ for escape of the system from this configuration point is sampled from the exponential distribution

$$\Theta(\tau) = \nu \exp(-\nu\tau) \quad (16)$$

in which ν is given by (15). The next step consists of choosing a particular reaction, which causes a transition of the system to another point. The probability p_α of selection of a chemical process α from the scheme (1)−(5) is proportional to the contribution of this reaction to the total rate ν of reactive collisions. That means

$$p_\alpha = \nu^{-1}\kappa_\alpha N_{\alpha 1} N_{\alpha 2} \tag{17}$$

where $N_{\alpha 1}$ and $N_{\alpha 2}$ denote populations of molecules of the corresponding two species involved in the bimolecular reaction α. After the reactive collision, the populations $\{N_V,N_U,N_E,N_X\}$ are updated as they result from the chosen reaction α. Given this new state, generation of dynamics proceeds beginning from the first step, and so on.

The periodically extended MD technique for reactive hard spheres[23] is applied as the second technique to simulate the time evolution of the system (1)−(5). The algorithm used here is exactly the same as described in ref 13, so we only mention the most essential aspects of the method. All reactants (E, R, S, U, V, X, and Y) are represented by hard spheres with the same mass (m) and diameter (d), which move according to classical mechanics. We assume that there are no thermal effects in reactions 1−5 so no kinetic energy is released or consumed when a reaction occurs and thus all collisions between spheres are elastic. The spheres are labeled by a chemical identity parameter which defines their "chemical" properties but does not have any influence on the mechanical motion. It implies that the system of spheres treated as a whole remains in the thermal equilibrium.

Both reactive and nonreactive collisions between spheres are considered. In order to control the rates of chemical processes, steric factors are introduced (they are denoted as s_i and s_{-i}, i = 1, 5). If a collision between spheres representing reagents of a particular process occurs, then a random number generator is called by the program and, if the obtained random number is smaller that the corresponding steric factor, then the collision is regarded as a reactive one. After such collision the chemical identity parameters of the spheres involved are modified according to the reaction scheme (1)−(5). Otherwise, the collision is nonreactive one and the spheres retain their chemical identities. A similar type of random selection of reactive collisions is commonly used in all large-scale microscopic simulations (including MD ones) of chemical systems.[10−19]

In order to keep the concentrations of the reactants R and S constant, we use the procedure described in ref 24. Beside the reactants, the system contains also nonreactive particles which play the role of reservoir of R and S molecules. If a particle of S (R) vanishes in one of the reactions, then simultaneously a randomly selected particle of reservoir is transformed into S (R), respectively. On the other hand, if a particle of S (R) appears, then a randomly chosen particle of S (R) becomes a particle of reservoir. These processes have no influence on the dynamics of the system because they do not participate in (1)−(5). However, the random transformations between the reservoir particles and reactants introduce a stirring in the simulated system which helps to destroy the nonequilibrium spatial correlations between molecules of reactants.[25]

To make the MD simulations efficient, we use a prerecorded trajectory representing a small system of spheres at the thermal equilibrium as the database on sequence of collisions. This trajectory is calculated as the solution of the Newton equations for all particles enclosed in a box with periodic boundary conditions. The information it contains completely describes the deterministic motion of hard spheres in a large system which is constructed by a periodic expansion of the original small one.[24] The periodic boundary conditions mean that positions and velocities of spheres are periodic in space with the period equal to the length of the box within which the system is enclosed. In this way the original small system may be periodically expanded in any of the directions by any integer number of the box lengths. Of course, if a chemical identity of molecules is neglected, then such expansion does not bring us any new information. However, the situation is different in a multicomponent chemical system, in which the motion of spheres is not related to chemical identity. First, different chemical composition may be initialized in various boxes by marking the equivalent (by periodicity) spheres in a different way. Secondly, steric factors (if they are not equal to unity) additionally differentiate the time evolution in various boxes, as a collision between the same objects may be reactive in one box and nonreactive in another. The periodic boundary conditions assure free motion of molecules between boxes. Therefore, having a recorded trajectory, one can use this information to get time evolutions for systems of various sizes.

The values of steric factors for MD simulations were obtained by scaling the phenomenological rate constants by 0.06(6), which leads to: $s_1 = 0.006(6)$, $s_{-1} = 0.008$, $s_{-2} = 0.006(6)$, $s_3 = 0.26$, $s_4 = 0.066(6)$, $s_{-4} = 0.266(6)$, $s_5 = 0.006(6)$, and $s_{-5} = 0.006(6)$ for reactions 1−5, respectively. For $k_2 = 8$ we have $s_2 = 0.533(3)$, whereas for $k_2 = 6$ the steric factor $s_2 = 0.4$. In order to adjust the frequencies of reactive collisions to the rate constants k_i appearing in the kinetic equations, the real time of the MD simulations t_{MD} is rescaled to the phenomenological time t according to:

$$t = \frac{1}{8} d^2 g \sqrt{\frac{\pi k_B T}{m}} \frac{s_1}{k_1} t_{MD} \tag{18}$$

where g is the value of the radial distribution function at the sphere diameter d for the system of spheres characterized by the assumed density, k_B is the Boltzmann constant, and T = 300 K is the temperature of our system. The results discussed in the next section have been obtained by a periodic expansion of the system of $N = 400$ hard spheres placed in a cubic box with the side length $l = 12.5d$ (and thus the packing fraction is $\eta \approx 0.11$ and $g = 1.35$). The prerecorded trajectory contained information on 20 160 000 collisions (over 50 000 collision per one sphere). It allowed us to study processes which in a phenomenological time scale last over $t_e \cong 840$. Having in mind that the phenomenological periods of oscillations are only slightly shorter than t_e, we see that the prerecorded trajectory covers times only slightly longer than one period. In order to study the long-time behavior of the system, we started a new simulation program from concentrations obtained at the end of the previous one. This procedure corresponds to the forced mixing of our system after each t_e interval, and it destroys possible spatial correlations which may appear between particles representing different reactants.

It is assumed that the density of the system is 8 mol/L, which corresponds to the volume of the original box equal to 83.(3) $\times 10^{-21}$ cm^3. At the beginning the chemical identities are assigned to spheres in a random way and all remaining spheres are marked as the reservoir particles.

The unit of volume is rescaled in the simulations to 10^3 cm^3/N = 1.6(6) $\times 10^{-21}$ cm^3, where N is the Avogadro number. Then the volume of the original box of MD is equal to 50 in these units. In the new units the number concentrations of reagents are numerically equal to the concentrations in moles/liter in the phenomenological equations. MD simulations performed for the system expanded by six box lengths in all directions give the volume Ω equal to 10 800, whereas the expansion by eight box lengths leads to Ω = 25 600.

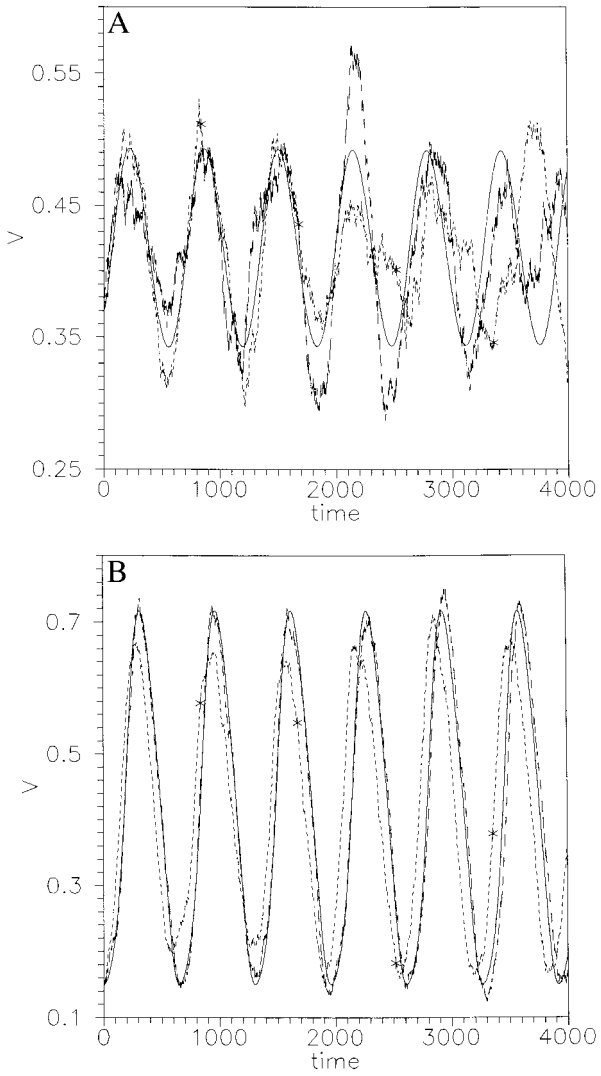

Figure 2. The concentration of V as a function of time for $\Omega = 10\,800$, $k_2 = 6$ (A) and $k_2 = 8$ (B) obtained in phenomenology (the solid line), ME calculations (long dashed line), and MD simulations (short dashed line). Stars mark the ends of intervals t_e which correspond to the length of individual simulation programs in MD simulations.

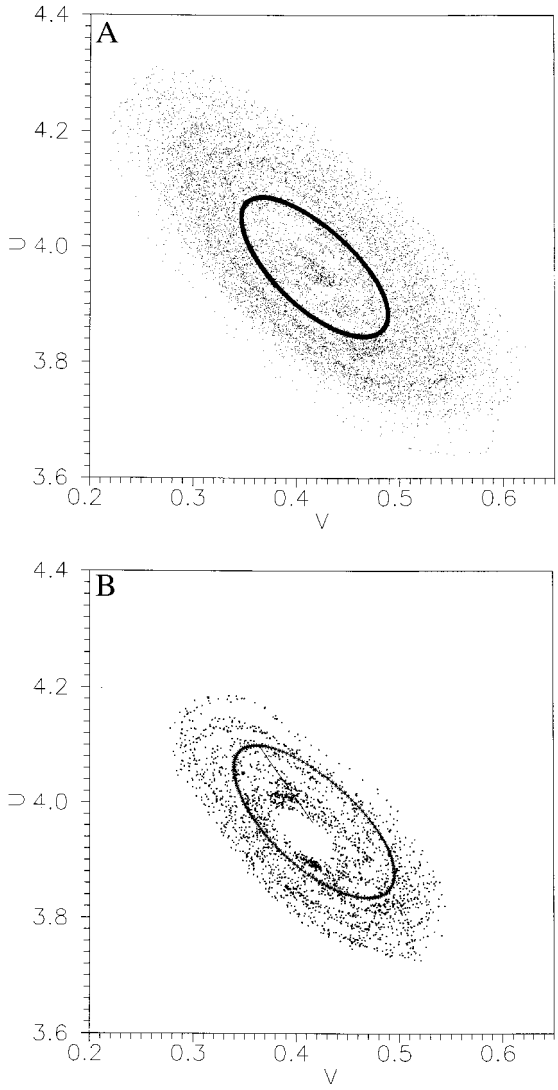

Figure 3. Comparison of the phenomenological limit cycle (thick line) with the results of simulations (points) for $k_2 = 6$ and $\Omega = 10\,800$; ME (A) and MD (B). In MD simulations the rate constants are scaled by 0.06(6). The thin straight line in (B) shows the direction of phase equal to zero.

IV. Results of Simulations

The initial condition for calculations presented below lies on the limit cycle. For $k_2 = 6$, they are $V(t = 0) = 0.366$, $U(t = 0) = 4.096$, $E(t = 0) = 0.018$, and $X(t = 0) = 0.095$; for $k_2 = 8$, $V(t = 0) = 0.150$, $U(t = 0) = 4.392$, $E(t = 0) = 0.039$, and $X(t = 0) = 0.117$. The concentration of V as a function of time for $\Omega = 10\,800$ at $k_2 = 6$ and $k_2 = 8$ obtained in phenomenology, ME calculations, and MD simulations are shown in Figure 2, A and B, respectively. Stars mark the ends of intervals t_e which correspond to the length of individual simulation programs in MD simulations. As predicted by the phenomenology, the results of the simulations exhibit oscillatory character of V. The oscillatory behavior is also observed for concentrations of all remaining reagents. The oscillations obtained for $k_2 = 8$ (Figure 2B) are more regular than those for $k_2 = 6$ (Figure 2A). As can be seen in Figure 2, fluctuations are more pronounced around the extrema. We have also observed that fluctuations of V are more important than those of U because the number of particles representing V is by an order of magnitude smaller than the number of U particles. Despite fluctuations the periods obtained in simulations (the average time between consecutive maxima of U) are in very good agreement with phenomenology and they are equal to $t_{ME} = 657$, $t_{MD} = 640$ for $k_2 = 6$, and $t_{ME} = 656$, $t_{MD} = 657$ for $k_2 = 8$. As expected for $\Omega = 25\,600$, oscillations appear to be more regular and the periods are in a better agreement with phenomenology.

In order to simplify the further comparison of the results obtained in simulations and phenomenology, we consider the projection of the four-dimensional limit cycle on the $V \times U$ phase plane. The projection of a trajectory obtained for $k_2 = 6$ and $\Omega = 10\,800$ (much longer than in Figure 2) on this plane is shown in Figure 3. The results obtained by both simulation methods are widely distributed around the limit cycle. In MD simulations the crater-like probability distribution can be noticed, whereas ME calculations give nonvanishing density of states near the center of the limit cycle. We have verified that the trajectories obtained in ME simulations approach the phenomenological limit cycle when the volume increases (compare Figure 4 for $\Omega = 3\,200\,000$).

There is a qualitative difference in the evolution of the system with $k_2 = 8$. The projection of a trajectory obtained for $\Omega = 10\,800$ is shown in Figure 5. In this case the trajectories occupy relatively narrow rings. It can also be noticed, in agreement

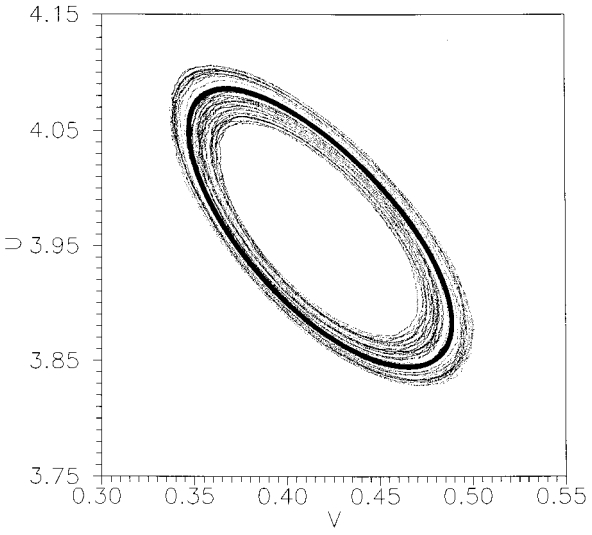

Figure 4. Comparison of the phenomenological limit cycle (thick line) with the results of ME simulations (the dashed line) for $k_2 = 6$ and large $\Omega = 3\,200\,000$.

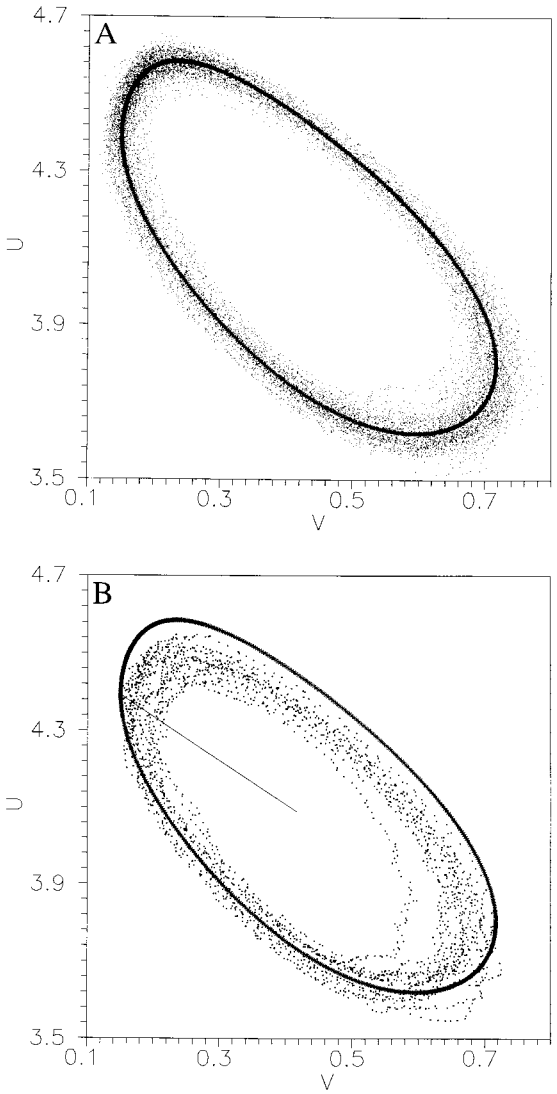

Figure 5. The same as in Figure 3 but $k_2 = 8$ and $\Omega = 10\,800$.

with Figure 2, that fluctuations are the strongest around the extrema and diminish with increase of volume. The ring obtained in ME simulations is focused around the phenomenological limit cycle. The left branch of phenomenological limit

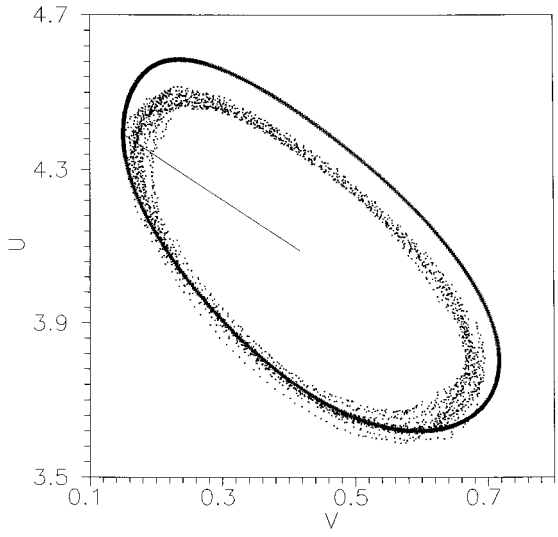

Figure 6. The same as in Figure 3B but $k_2 = 8$ and $\Omega = 25\,600$.

cycle agrees well with the results of MD simulations (see Figure 5B). However, the right part of MD results is shifted toward smaller concentrations of V as compared with the phenomenological limit cycle. The qualitative difference between the phenomenological limit cycle and MD does not change if the size of system increases; it can be seen even more clearly in Figure 6 which shows the results for $\Omega = 25\,600$. To get more information on the origin of this effect, we performed additional MD simulations for lower relative frequency of reactive collisions (the rate constants were scaled by 0.02). We observe that the right branch of the trajectory is shifted toward the phenomenological limit cycle. Therefore, we believe that the difference comes from the nonequilibrium effects related to spatial correlations between concentrations of reactants which become less important if the reactions are slower.[25] The analogous nonequilibrium effect for $k_2 = 6$ is probably hidden by very large fluctuations.

In the sequel we shall describe the results of simulations using a phase and a radius. Let us define the center C of the projected limit cycle as the point on the $V \times U$ plane, the coordinates of which are the average values of concentrations. The phenomenology gives the following coordinates of C:

$$V_c = 0.416\,565,\ U_c = 3.964\,75,\ \text{for } k_2 = 6$$

$$V_c = 0.416\,609,\ U_c = 4.089\,82 \text{ for } k_2 = 8$$

The limit cycles obtained in ME simulatins are in such good agreement with the phenomenological ones that we have not introduced separate centers for them and used the phenomenological values. Having in mind that the MD results are shifted with respect to the phenomenological limit cycle, we have introduced separately the center of MD limit cycle (C_{MD}) as the mean of U and V obtained in simulations. The coordinates of C_{MD} are:

$$U_c = 3.933, V_c = 0.414 \text{ for } k_2 = 6 \text{ and } \Omega = 10\,800$$

$$U_c = 4.048, V_c = 0.413 \text{ for } k_2 = 8 \text{ and } \Omega = 10\,800$$

$$U_c = 3.934, V_c = 0.414 \text{ for } k_2 = 6 \text{ and } \Omega = 25\,600$$

$$U_c = 4.046, V_c = 0.412 \text{ for } k_2 = 8 \text{ and } \Omega = 25\,600$$

It is noteworthy that the MD results are in a fair agreement with the phenomenological position of the center. The changes

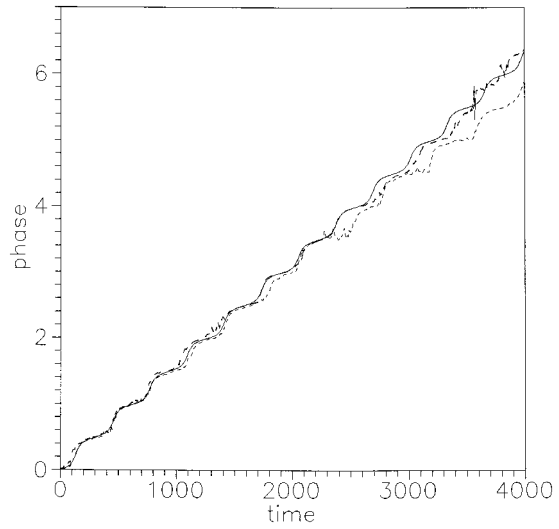

Figure 7. Comparison of phases as functions of time for $k_2 = 6$ and $\Omega = 10\,800$: phenomenology (solid line), ME calculations (long-dashed line), and MD simulations (short-dashed line).

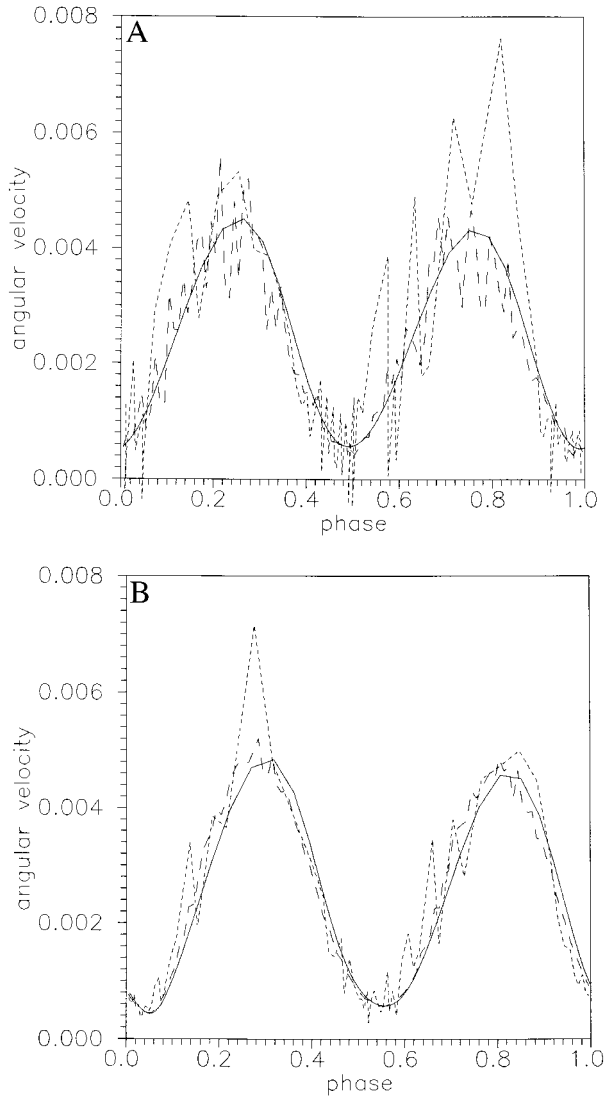

Figure 8. Comparison of angular velocities as functions of the phase for $k_2 = 6$, $\Omega = 10\,800$ (A) and $k_2 = 8$, and $\Omega = 10\,800$ (B). Notation as in Figure 7.

in coordinates of C for $k_2 = 6$ and $k_2 = 8$ predicted by the phenomenology are confirmed by the MD simulations. Moreover, C_{MD} obtained for both sizes of the system agree very well.

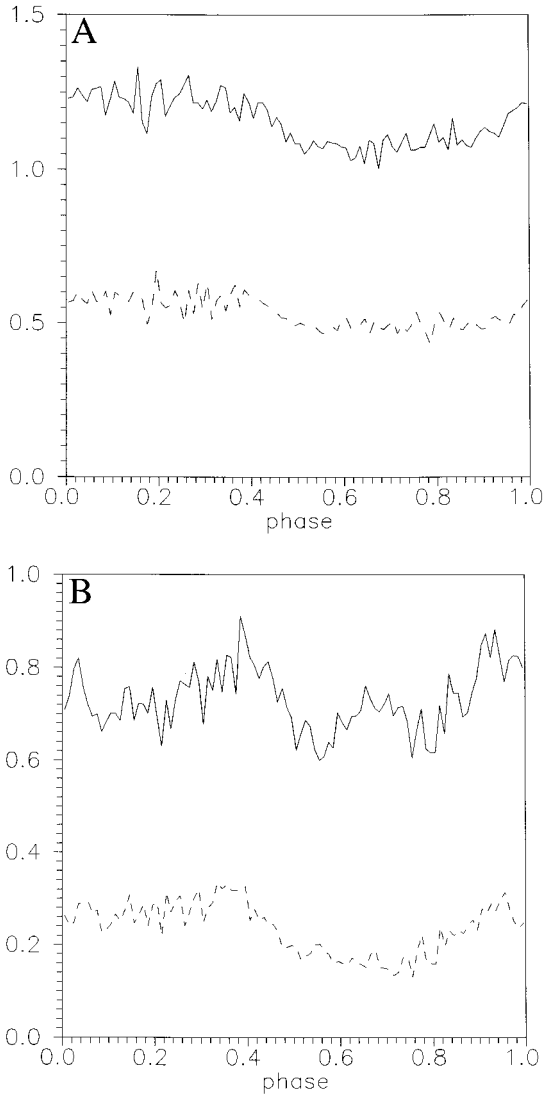

Figure 9. The radius (solid line) and its dispersion (dashed line) as functions of the phase for $k_2 = 6$ and $\Omega = 25\,600$: (A) ME calculations and (B) MD simulations.

Knowing the center of the projected limit cycle, we can introduce parameterization of the cycle using radius and phase. The radius is defined as the length of vector from the center toward a given point on the cycle. To define the phase one needs to specify the direction on the plane which corresponds to the zero phase. In our analysis it is the direction from the center C toward the point P_0 which represents the initial state of simulation. For $k_2 = 6$ it was $V_0 = 0.366$ and $U_0 = 4.096$, whereas for $k_2 = 8$ we set $V_0 = 0.150$ and $U_0 = 4.392$. The phase for any point Q can be calculated as the angle between vectors $\vec{CP}_0$ and $\vec{CQ}$. The phase is positive for the clockwise direction, because the system rotates in this direction. In the following we use the scaled phase that is the above-defined angle divided by 2π. In this way the phenomenological radius is a well-defined function of the phase ϕ. More generally, any point Q on the plane $V \times U$ is localized by two coordinates: phase ϕ, and the scaled radius defined as the ratio of the distance CQ to the radius of the projected limit cycle for the same phase.

Comparison of $\phi(t)$ obtained from simulations and phenomenology for the case $k_2 = 6$ is presented in Figure 7. The considered range of times was selected in order to see what is the influence of well-pronounced fluctuations in $U(t)$ and $V(t)$ (cf. Figure 3) on $\phi(t)$. It can be seen that within a single period the phase as a function of time has two regions of slow increase,

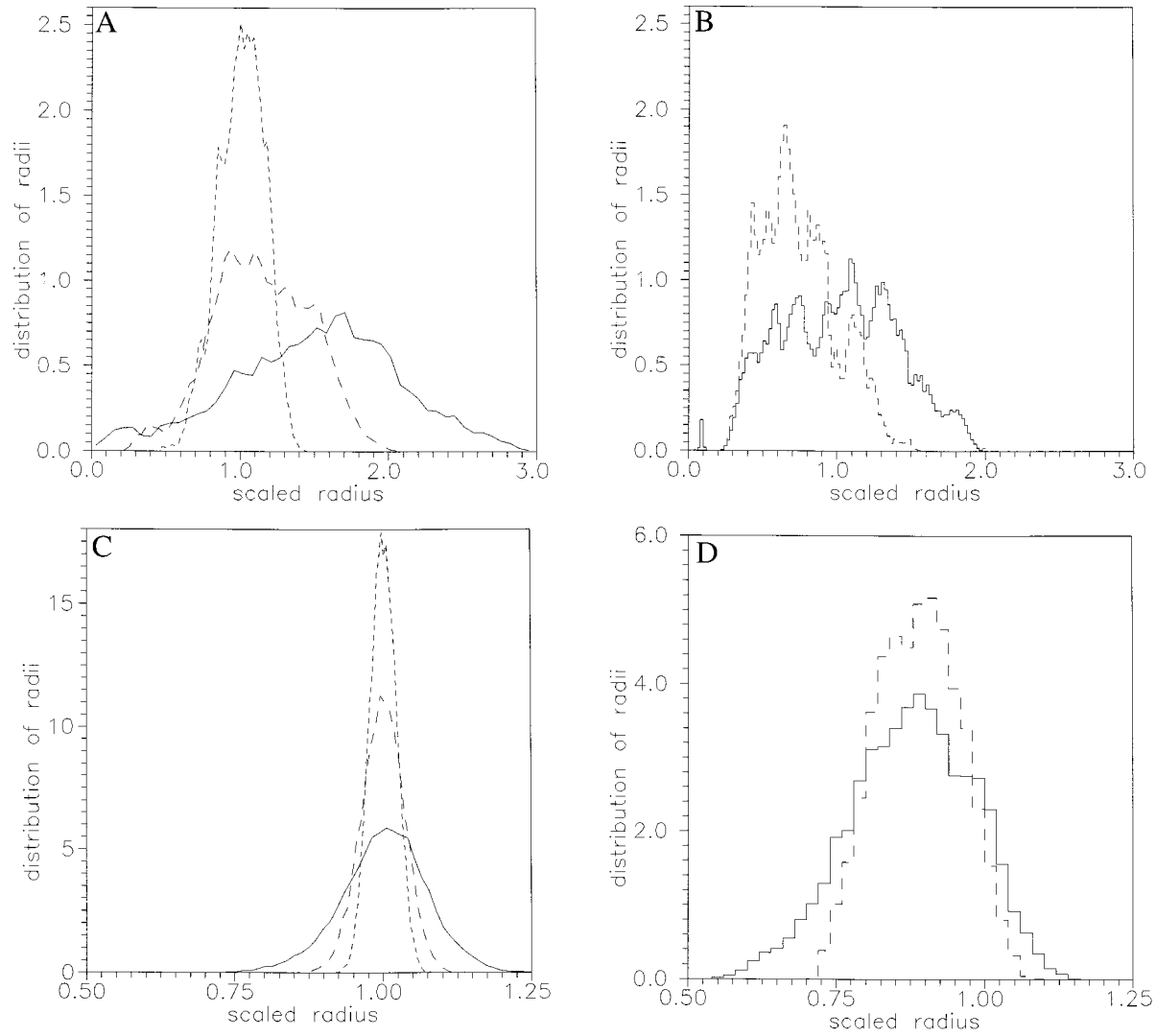

Figure 10. The distribution functions of the radius. (A) ME results for $k_2 = 6$ and $\Omega = 10\,800$ (solid line), $\Omega = 86\,400$ (long-dashed line), and $\Omega = 691\,200$ (short-dashed line). (B) MD results for $k_2 = 6$ and $\Omega = 10\,800$ (solid line) and $\Omega = 25\,600$ (dashed line). (C) ME results for $k_2 = 8$ and $\Omega = 10\,800$ (solid line), $\Omega = 50\,000$ (long-dashed line), and $\Omega = 204\,800$ (short-dashed line). (D) ME results for $k_2 = 8$ and $\Omega = 10\,800$ (solid line) and $\Omega = 25\,600$ (dashed line).

which correspond to the extrema of $U(t)$, and two regions of fast increase related to the intervals of time in which $U(t)$ changes rapidly. The intervals in which fluctuations are pronounced correspond to the intervals in which the phase is nearly constant. Each plateau of the phase increases the difference between $\phi(t)$ obtained in simulations and the phenomenological one. We note that for $k_2 = 8$ there is much better agreement between the results obtained by all three methods. In this case small shifts of ϕ with respect to the phenomenological phase appear only in regions where ϕ changes slowly.

The influence of fluctuations can be seen more clearly if we consider the angular velocity. The results obtained for MD and ME simulations are compared with phenomenology in Figure 8A,B for $k_2 = 6$ and $k_2 = 8$, respectively, and $\Omega = 10\,800$. In MD simulations we record approximately 7000 points of trajectory $(V(t), U(t))$ per single period. They are grouped into sets consisting of 100 points, and the angular velocity $\omega(\phi) = d\phi/dt$ is separately calculated for each group. The angular velocity has two maxima per period and the values of $\omega(\phi)$ change by an order of magnitude. For $k_2 = 8$ (Figure 8B), we have good agreement between the phenomenological $\omega(\phi)$ and the results of MD simulations. In the case of $k_2 = 6$ (see Figure 8A), the agreement is also good but the dispersion is much larger. The influence of fluctuations on the angular velocity is the most important in the intervals of time for which ω increases.

Figure 9A,B shows the scaled radius and its dispersion obtained in simulations as functions of the phase for $k_2 = 6$ and $\Omega = 25\,600$. There is a qualitative agreement between ME results (see Figure 9A) and MD data (Figure 9B). However, the radius of the MD trajectory is smaller than the ME one (compare Figure 5). Note that the dispersion obtained from ME simulations is larger than that from MD.

The distribution functions of all relative radii obtained in simulations are shown in Figure 10A−D. For MD simulations, the radius is calculated with respect to C_{MD} and it is scaled by the phenomenological radius corresponding to the same phase. As expected, the dispersion of distribution functions decrease with increasing volume. Figure 10A presents the results obtained from ME for $k_2 = 6$ and various volumes Ω. The corresponding results obtained from MD are shown in Figure 10B. In both cases the average radius for small systems is larger than the phenomenological one. In ME simulations the mean value of the radius converges to the phenomenological result if Ω increases. For systems of the same size, the dispersions of the radius in ME simulations are larger than those observed in

MD. Figure 10C,D shows the distributions of radii for $k_2 = 8$ obtained in ME and MD simulations, respectively. In this case the distribution functions are much narrower than for $k_2 = 6$. The results of ME simulations agree with phenomenology because the maximum of the distributions is close to 1 and its does not depend on Ω. The MD results give smaller values of the average radius than ME simulations. This tendency is similar to the effect mentioned above for $k_2 = 6$, and comes from the influence of the nonequilibrium effect on the shape of MD trajectories. It can be expected for large volumes that dispersions scale like $\Omega^{-1/2}$; however, we do not observe such scaling in the range of volumes ($\Omega < 700\,000$) studied in ME simulations.

V. Discussion

The results of our simulations exhibit oscillatory behavior for the model of chemical system as it is predicted by phenomenological equations. The periods of oscillations obtained from simulations are in a good agreement with their phenomenological values. However, instead of a closed line corresponding to the limit cycle, the trajectories obtained in simulations are dispersed as a "ring"-like structure describing the behavior of the system influenced by internal fluctuations. We introduced an approximate quantitative description of fluctuations based on the radius and the phase. As expected, we have found that the strength of fluctuations decreases with the system's size. By considering two cases in which (according to the phenomenology) the limit cycle is weakly and strongly attractive, we have been able to distinguish two types of fluctuations, which have not been discussed separately in the literature yet. Short time scale fluctuations are related to stochasticity in elementary reaction steps and long time fluctuations correspond to random motion of the simulated trajectories in the phase space. The later ones depend on phenomenological parameters (k_2 in our case). In order to see more clearly the difference between these types of fluctuations, we compared the average dispersion of radius for time intervals which are one period long with the dispersion for the whole simulation. For $k_2 = 8$ the average dispersion is about two-thirds the total dispersion. For $k_2 = 6$ the average dispersion of radii measured within a single period is less than half. It indicates that in the oscillating system with strongly attracting limit cycle ($k_2 = 8$) fluctuations are fully developed at much shorter times (as compared with the period of oscillations) than in the case where the limit cycle is weakly attracting ($k_2 = 6$).

Nonequilibrium effects which are clearly seen for $k_2 = 8$ may be connected with spatial correlations which disturb homogeneity of the system.[25] These effects decrease the effective value of k_2 as compared with the phenomenological one. The influence of k_2 on a position of the limit cycle can be easily seen on the projection of the limit cycle on the plane $E \times X$. The projections for $k_2 = 6$ and $k_2 = 8$ are shown in Figure 11. As can be seen the projection of the MD trajectory for $k_2 = 8$, shown as points, is shifted down and left to what corresponds to a smaller effective value of this rate constant.

The model constructed in this paper is composed of elementary bimolecular reactions and, therefore, it allows direct comparison of the results of MD and ME simulations. We have found that the ME results are in a good agreement with the more rigorous MD method. The good agreement between the both methods obtained in our simulations confirms earlier results of Baras et al.[26] who compared the ME approach with the Bird's technique for another model of an oscillating system. We can expect even better agreement when the considered reactions are slower, so that the nonequilibrium effects are less important. In such cases the ME approach can give a reasonable description of global fluctuations in oscillating systems. However, more rigorous techniques like MD may be required to describe local fluctuations which can strongly influence the dynamics of nonideally stirred (or unstirred) macroscopic, nonlinear systems.

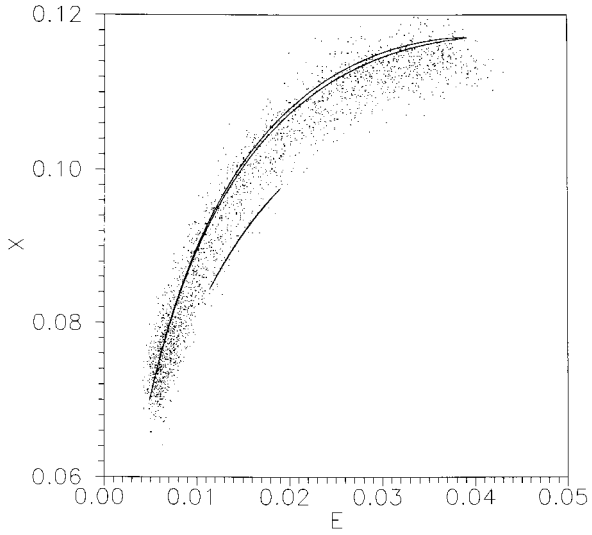

Figure 11. The projection of trajectories on the plane $E \times X$. The upper solid line shows the cycle for $k_2 = 8$ and the lower one for $k_2 = 6$. Points denote the MD trajectory for $k_2 = 8$ and $\Omega = 10\,800$. In MD simulations the rate constants are scaled by 0.06(6).

Acknowledgment. This work was supported by Grant KBN 3T09A 120 08 provided by the Polish State Committee for Scientific Research.

References and Notes

(1) See, for example: Zhabotinsky, A. M. *Concentrations Autooscillations*; Nauka: Moscow, 1974 (in Russian). Field, R. J.; Burger, M. *Oscillations and Travelling Waves in Chemical Systems*; Wiley: New York, 1985. Kawczyński, A. L. *Chemical Reactions from Equilibrium through Dissipative Structures to Chaos*; WN-T: Warsaw, 1990 (in Polish). Field, R. J.; Gyorgyi, L. *Chaos in Chemistry and Biochemistry*; World Scientific: Singapore, 1993.

(2) Nicolis, G.; Prigogine, I. *Self-Organization in Non-equilibrium Systems*; Wiley: New York, 1977.

(3) Zhabotinsky, A. M. In *Oscillatory Processes in Biological and Chemical Systems*; Nauka: Moscow, 1967; p 149 (in Russian).

(4) Ali, F.; Menzinger, M. *J. Phys. Chem.* **1997**, *101*, 2304 and references therein.

(5) Zaikin, A. N.; Zhabotinsky, A. M. *Nature* **1970**, *225*, 535.

(6) Zaikin, A. N.; Kawczyński, A. L. *J. Non-Equil. Thermodyn.* **1977**, *2*, 39.

(7) van Kampen, N. G. *Stochastic Processes in Physics and Chemistry*; North-Holland: Amsterdam, 1983.

(8) Gardiner, C. W. *Handbook of Stochastic Methods*; Springer-Verlag: Berlin, 1985.

(9) Allen, M. P.; Tidesley, D. J. *Computer Simulations of Liquids*; Clarendon Press: Oxford, 1987.

(10) Gorecki, J.; Gryko, J. *Comput. Phys. Commun.* **1989**, *54*, 245.

(11) Gesshirt, K.; Praestgaard, E.; Toxvaerd, S. *J. Chem. Phys.* **1997**, *107*, 9406 and references therein.

(12) Kawczyński, A.L.; Nowakowski, B. *Pol. J. Chem.* **1996**, *70*, 1468.

(13) Gorecki, J.; Kawczyński, A. L.; Nowakowski, B. *Pol. J. Chem.* **1997**, *71*, 244.

(14) Frankowicz, M.; Kawczyński, A. L. *Pol. J. Chem.* **1997**, *71*, 467.

(15) Baras, F.; Malek Mansour, M. *Adv. Chem. Phys.* **1997**, *100*, 393 and references therein.

(16) Gorecki, J.: Kawczyński, A. L. *J. Chem. Phys.* **1990**, *92*, 7546.

(17) Kawczyński, A. L.; Gorecki, J. *J. Phys. Chem.* **1992**, *96*, 1060. Mareschal, M.; De Wit, A. *J. Chem. Phys.* **1992**, *96*, 2000. Malek-Mansour, M.; Baras, F. *Physica A* **1992**, *188*, 253. Xiao-Guang, W.; Kapral, R. *J. Chem. Phys.* **1994**, *100*, 5936.

(18) Kawczyński, A. L.; Gorecki, J. *J. Phys. Chem.* **1993**, *97*, 10358.

(19) Gorecki, J.; Kawczyński, A. L. *J. Phys. Chem.* **1996**, *100*, 19371.

(20) Tikhonov, A. N. *Mat. Sbor*. **1952**, *31*, 574 (in Russian).
(21) Richter, P. H.; Proccacia, I.; Ross, J. *Adv. Chem. Phys.* **1980**, *43*, 217.
(22) Gillespie, D. T. *J. Phys. Chem.* **1977**, *81*, 2340.
(23) Gorecki, J. *Mol. Phys. Rep.* **1995**, *10*, 48.
(24) Boissonade, J. *Physica A* **1982**, *113A*, 607.
(25) Kuramoto, Y. *Prog. Theor. Phys.* **1974**, *52*, 711. Nicolis, G.; Malek Mansour, M. *Phys. Rev.* **1984**, *29A*, 2845. Kitahara, K.; Seki, K.; Suzuki, S. *J. Phys. Soc. Jpn.* **1990**, *59*, 2309. Gorecki, J.; Kitahara, K. *Physica A* **1997**, *245A*, 164.
(26) Baras, F.; Pearson J. E.; Malek Mansour, M. *J. Chem. Phys.* **1990**, *93*, 5747.